Kinetic Pathways for the Isotropic-Nematic Phase Transition in a System of Colloidal Hard Rods: A Simulation Study

Alejandro Cuetos and Marjolein Dijkstra

Soft Condensed Matter, Utrecht University, Princetonplein 5, 3584 CC Utrecht, The Netherlands

(Received 14 November 2006; published 26 February 2007)

We study the kinetic pathways for the isotropic-to-nematic transition in a fluid of colloidal hard rods. In order to follow the formation of the nematic phase, we develop a new cluster criterion that distinguishes nematic clusters from the isotropic phase. Applying this criterion in Monte Carlo simulations, we find spinodal decomposition as well as nucleation and growth depending on the supersaturation. We determine the height of the nucleation barrier and we study the shape and structure of the cluster. More specifically, we find ellipsoidal nematic clusters with an aspect ratio of about 1.7 and a homogeneous nematic director field. Our results are consistent with theoretical predictions on the shape and director field of nematic tactoids. Classical nucleation theory gives reasonable predictions for the height of the nucleation barrier and the critical nucleus size.

DOI: 10.1103/PhysRevLett.98.095701 PACS numbers: 64.60.Qb, 64.70.Md, 82.70.Dd

The kinetics of phase transitions in systems of *nonspherical* particles is poorly understood, even for the relatively simple isotropic-to-nematic (IN) transition of uniaxial hard rods. Recent experiments with supersaturated suspensions of colloidal rods show a rich phenomenology, which involves a nucleation-and-growth regime as well as a spinodal decomposition regime, depending on the degree of supersaturation [1–5]. Moreover, nonspherical nematic droplets (so-called tactoids) that grow with time at the expense of their isotropic environment have been observed. Despite these recent new results there are many remaining questions. How high is the nucleation barrier that is to be crossed during this process, what is the shape of the critical nucleus at the top of the barrier? How does all this depend on the supersaturation and on the length of the rods? Questions like these have so far not been answered, neither experimentally, since one can only detect macroscopically large (postcritical) nematic droplets that exist when phase separation is almost completed [1–5], nor theoretically, since classical nucleation theory predicts a diverging barrier height and critical nucleus size for infinitely long rods (see below). Surprisingly, perhaps, also computer simulations have so far not been able to shed any light on this subject, even though a substantial recent progress in our understanding of gas-liquid and fluid-crystal nucleation of *spherical* particles is due to Monte Carlo (MC) simulations [6–8]. Applying simulation techniques to study nucleation of rods has been prohibited by problems to formulate an appropriate cluster criterion that is able to identify nematic clusters in an isotropic phase [9].

In this Letter, we develop a new cluster criterion that distinguishes nematic clusters from the isotropic phase. Employing this criterion, we are able to study for the first time the kinetic pathways of the IN transition in a suspension of colloidal rods, modeled by hard spherocylinders (HSC) with diameter σ and length L. We perform MC simulations of colloidal hard rods with $L^* = L/\sigma = 5$ and $L^* = 15$ in a rectangular box with periodic boundary conditions. These systems show a phase transition from an isotropic fluid phase to an orientationally ordered nematic phase at a pressure $P^*_{\mathrm{IN}} = 1.117$ for $L^* = 5$ ($P^* = \beta P \sigma^3$, $\beta = 1/k_B T$, where k_B is Boltzmann's constant, and T the temperature), and at $P^*_{\mathrm{IN}} = 0.097$ for $L^* = 15$ [10]. For $L^* = 5$, the transition is weakly first order without a clear density jump [10]. For $L^* = 15$ the I-N transition is of first order with a density jump of about 20%.

In order to follow the formation of the nematic phase from the isotropic fluid phase in MC simulations, we need a cluster criterion that identifies the nematic clusters. To this end, we first make a distinction between particles that have a nematiclike and an isotropiclike environment. Particle i is nematiclike if its local environment has an orientational order significantly larger than in an isotropic phase. The local environment of particle i is defined by all particles j with a surface-to-surface distance $\rho_{ij} \leq 1.5\sigma$ such that this local environment is not defined by only the nearest neighbors, but also by the next-nearest neighbors, thereby taking advantage of the long-ranged orientational order in the nematic phase. The local orientational order of particle i is defined by

$$S(i) = \frac{1}{n_i} \sum_{j=1}^{n_i} \left(\frac{3}{2} |\mathbf{u}_j \cdot \mathbf{u}_i|^2 - \frac{1}{2} \right), \tag{1}$$

where $\mathbf{u}_j$ is the unit orientation vector of particle j and n_i the number of particles with $\rho_{ij} \leq 1.5\sigma$. We have adopted the cluster criterion that particle i is nematiclike if $S(i) > 0.4$. After identifying the nematic particles in the system, we determine the nematic clusters by the criterion that two nematic particles i and j belong to the same cluster if (i) $\rho_{ij} < 0.5\sigma$ and (ii) the dot product $|\mathbf{u}_i \cdot \mathbf{u}_j| > 0.85$. Applying this cluster criterion, we find independently of rod length only a small number of very small nematic clusters (<5% of all particles) in the coexisting bulk isotropic phase and a single big nematic cluster in the nematic phase.

We now employ this cluster criterion to study the transition pathways of the IN transition. To this end, we compress an isotropic fluid of $N = 8640$ particles at $\Delta P^* = P^*/P^*_{\mathrm{IN}} - 1 = 0.137$ for $L^* = 5$ using MC simulations in the isobaric-isothermal ensemble. As shown in Ref. [11], both molecular dynamics and MC simulations can be used to sample the transition pathways. We note that we only used translational and rotational moves in our MC simulations and no unphysical ones like cluster moves, which allow us to sample the most probable and realistic pathways. At this pressure, we find that the isotropic phase transforms spontaneously into a nematic phase. Upon compressing the isotropic phase, the density of the system increases gradually and we are not able to find a state on the metastable isotropic fluid branch. We find that phase separation sets in immediately after compressing as many small nematic clusters are formed throughout the system [Fig. 1(a)]. These clusters grow until they coalesce to form an interconnected ''labyrinth structure'' [Fig. 1(b)]. The nematic order parameter of this interconnected structure is small as the orientations of the original clusters of this labyrinth structure are very different. Subsequently, the nematic order parameter of the labyrinth structure increases as the clusters reorient. The immediate phase separation and the formation of a labyrinth structure is typical for spinodal decomposition. At this pressure, the isotropic phase is unstable. At lower supersaturations, one might expect to find the nucleation-and-growth regime. We were, however, unable to find any metastable isotropic fluid branch or nucleation-and-growth phenomenon for $L^* = 5$. This might be explained by the weak first-order character of the transition and the short metastable isotropic fluid branch [10].

We now turn our attention to $L^* = 15$, for which the IN transition is strongly first order [10]. We first compress the isotropic fluid phase of $N = 4320$ particles beyond coexistence to $\Delta P^* = 0.289$. At this supersaturation, the isotropic phase is unstable and we observe spontaneous formation of the nematic phase. We again find all the characteristics of spinodal decomposition. Figure 2(a) shows the size of the biggest cluster in the system identified by our cluster criterion, the nematic order parameter of this cluster, and the global nematic order parameter as a function of the number of MC cycles. The nematic order parameter is defined by the largest eigenvalue of the standard 3×3 nematic order parameter tensor. In the initial stage of phase separation, we find that many small nematic clusters appear throughout the system with a high nematic order. After about 1×10^5 MC cycles, the nematic clusters coalesce and form an interconnected cluster: the nematic order parameter of this cluster drops suddenly as the original clusters have different orientations. Subsequently, the size and the nematic order of this interconnected cluster grow gradually until the whole system is transformed into the nematic phase. The observed phase separation process has all the typical features of spinodal decomposition and is similar to the behavior described for $L^* = 5$.

Next we compress the system at a lower supersaturation of $\Delta P^* = 0.082$. We again observe that the isotropic phase transforms spontaneously into the nematic phase. However, at this pressure, we observe all the characteristics of nucleation and growth. Upon compressing the system, we find that the system remains for a very long time in a metastable isotropic fluid phase at a density $\rho^* = \rho\sigma^3 = 0.147$, slightly above the coexisting density of the isotropic fluid phase $\rho^*_I = 0.144$. Along the simulation, small nematic clusters are formed but they also disappear. After a certain number of MC steps, a single nematic cluster starts to grow. Figure 2(b) shows that the size of this single cluster grows gradually and that the nematic order of this cluster remains nearly constant. It is evident from Fig. 2 that the global nematic order parameter follows the growth of the nematic cluster. The long period that the system stays in a metastable isotropic fluid phase and the induction time before a single cluster starts to grow is typical for nucleation and growth.

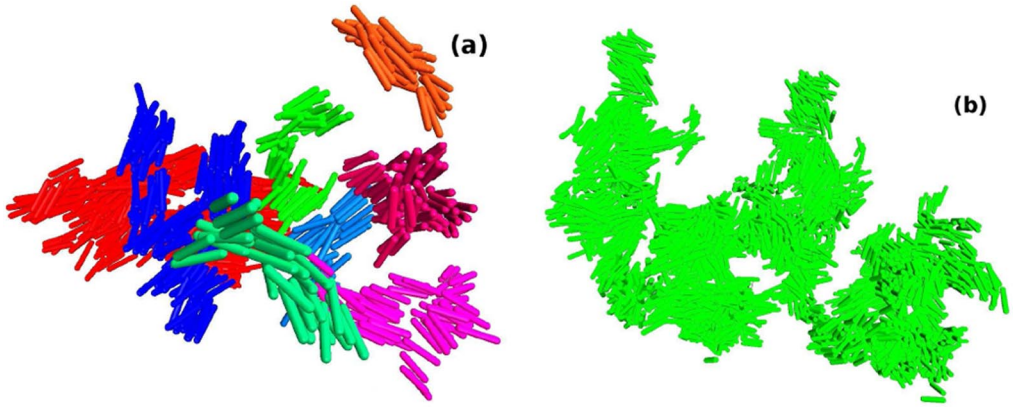

FIG. 1 (color online). Typical intermediate configurations in the IN transition for a HSC fluid with $L^* = 5$ at $\Delta P^* = 0.137$. (a) Many small clusters with number of particles $n = 462$ (red), 115 (blue), 69 (pink), 60 (light pink), 49 (light blue), 40 (orange), 34 (green), and 32 (light green) are formed in the initial stage of spinodal decomposition. (b) In a later stage these clusters coalesce and form an interconnected labyrinth structure.

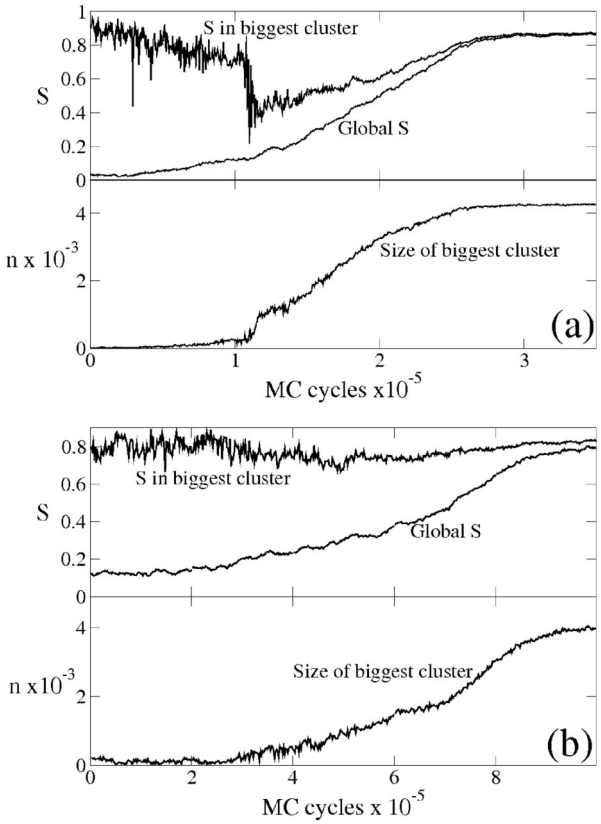

FIG. 2. Evolution of the size of the biggest cluster n in the system (bottom panels), the nematic order parameter S of the biggest cluster and of the total system (top panels), for a HSC fluid with $L^* = 15$ at (a) $\Delta P^* = 0.289$ in the spinodal decomposition regime, and (b) $\Delta P^* = 0.082$ in the nucleation-and-growth regime.

At lower supersaturation $\Delta P^* \leq 0.07$, spontaneous nucleation never occurred on the time scales of our simulations. However, at these pressures, we can study the height of the nucleation barrier and the structure of the nematic clusters using the umbrella sampling technique [6,7,9]. This technique allows us to bias the sampling to configurations containing clusters with a certain size. Using this technique, we measure the equilibrium probability $P(n)$ to find a cluster of n rods. The Gibbs free energy of a nematic cluster of size n is given by $\beta\Delta G(n) = -\ln P(n)$, which we compute for $\Delta P^* = 0.041$, 0.052, and 0.062, as shown in Fig. 3. The top of the barrier determines the Gibbs free energy of the critical cluster ΔG_{crit} and its critical size is n_{crit}. For $\Delta P^* = 0.041$ clusters with $n > 145$ start to percolate and it is therefore impossible to calculate the barrier height and the critical nucleus size. We note that the calculation of the present Gibbs free energy curve took more than 4 months of CPU time on a desktop PC. We can conclude that the height of the barrier is $\beta\Delta G_{\text{crit}} > 25$ and $n_{\text{crit}} > 145$. For $\Delta P^* = 0.052$, we find $\beta\Delta G_{\text{crit}} \approx 19.5$ with $n_{\text{crit}} \approx 95$, while for $\Delta P^* = 0.062$, $\beta\Delta G_{\text{crit}} \approx 16.0$ with $n_{\text{crit}} \approx 83$.

Next we study the shape and the structure of the nematic cluster as a function of its size using umbrella sampling.

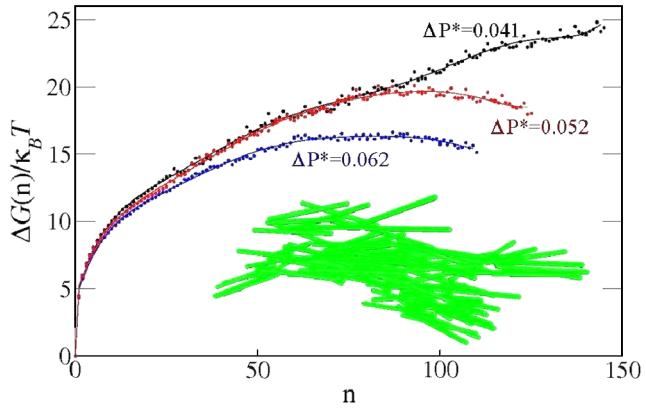

FIG. 3 (color online). Gibbs free energy of a HSC fluid with $L^* = 15$ as a function of the nematic cluster size n at supersaturation $\Delta P^* = 0.041$, 0.052, and 0.062. As a guide to the eye we have fitted the barrier with an 8th degree polynomial. The inset shows a typical configuration of a critical cluster ($n = 95$) for $\Delta P^* = 0.052$.

Contour plots of the density profiles $\rho^*(z, r)$ of the nematic particles in the cluster are shown in Fig. 4 as a function of the distance from the center-of-mass of the cluster in the direction parallel (z) and perpendicular (r) to the nematic director. We show profiles for a critical cluster ($n = 95$) and for a precritical one ($n = 20$) for $P^* = 0.102$. The density profiles show that the shape of the nematic cluster is ellipsoidal with the long axis parallel to the nematic director. The aspect ratio of the clusters are $z_{\max}/r_{\max} = 1.7 \pm 0.3$. We also find ellipsoidal symmetry for the density profile inside the cluster with a density decreasing gradually from the center to the surface of the cluster.

We also plot the nematic order parameter profile $S(z, r)$ of all the particles (isotropic and nematic). The nematic order parameter is defined by the second Legendre polynomial $S = \langle(3|\mathbf{u}_i \cdot \mathbf{n}|^2 - 1)/2\rangle$, where $\mathbf{n}$ is the nematic director of the cluster. Upon closer inspection of $S(z, r)$, we observe a homogeneous director field inside the cluster. This is also supported by the striking similarities that we find for the shape and aspect ratio of the contour plots for $\rho^*(z, r)$ and $S(z, r)$. The value of the nematic order parameter at the center of the cluster is ≈ 0.8, which is consistent with the nematic order parameter of the corresponding bulk nematic phase, and decays slowly from the center to the surface of the cluster.

We now compare our results with a recent theoretical study based on a minimization of the free energy of a macroscopic nematic droplet [12]. Because of a competition between the interfacial tension, the anchoring strength, and bulk elasticity, this theory predicts different morphologies of nematic tactoids as a function of a dimensionless elastic stiffness $\kappa \equiv K/\gamma V^{1/3}$ and dimensionless anchoring strength ω, where K denotes the Frank elastic constant, γ the interfacial tension, and V the volume of the droplet. Using values from Onsager theory for K, ω, and γ [13,14], we find $\omega \simeq 0.6$ and $\kappa \gg 1$ with V equal to the size of our

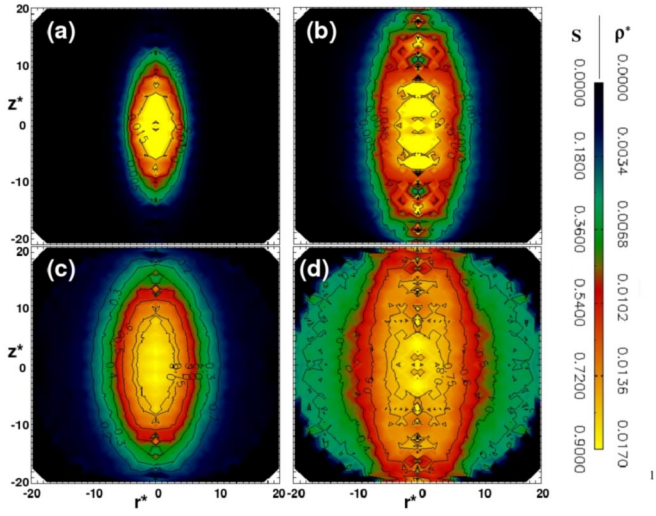

FIG. 4 (color online). Contour plots for the density [(a),(b)] and nematic order parameter [(c),(d)] as a function of the distance from the center of mass of the cluster in the direction parallel ($z^* = z/\sigma$) and perpendicular ($r^* = r/\sigma$) to the nematic director for a critical cluster of size $n = 95$ [(b),(d)] and for a precritical cluster of size $n = 20$ [(a),(c)] at $\Delta P^* = 0.052$ in a HSC fluid with $L^* = 15$.

critical cluster. For these values the theory predicts homogeneous spheroidal (ellipsoidal) droplets with an aspect ratio of $1 + \omega \simeq 1.6$. Our results on (i) the shape of the critical cluster, (ii) the aspect ratio, and (iii) the homogeneous director field are in excellent agreement with these theoretical predictions.

We also compare our results with classical nucleation theory (CNT). According to CNT, the Gibbs free energy of a *spherical* nucleus with radius R reads $\Delta G(n) = 4\pi R^2\gamma - 4\pi R^3\rho_N|\Delta\mu|/3$ with ρ_N the number density of the coexisting nematic phase and $\Delta\mu < 0$ the difference in chemical potential of the nematic and isotropic phase. The maximum height of the nucleation barrier is given by $\Delta G_{\rm crit} = 16\pi\gamma^3/3(\rho_N\Delta\mu)^2$ with a critical nucleus radius $R_{\rm crit} = 2\gamma/\rho_N|\Delta\mu|$. Using $\beta\gamma L\sigma = 0.183$ and $\rho_N L^2\sigma = 5.431$ from Onsager theory [13], we find $\beta\Delta G_{\rm crit} \simeq (0.0035/|\beta\Delta\mu|^2)L/\sigma$ and $R_{\rm crit} \simeq (0.067/|\beta\Delta\mu|)L$. In the Onsager limit $L^* \to \infty$ both $\beta\Delta G_{\rm crit}$ and $R_{\rm crit}$ diverge. For $L^* = 15$, however, we find using Onsager theory that $\Delta P^* = 0.041$, 0.052, 0.062 correspond with $\beta\Delta\mu = 0.041$, 0.052, 0.063, respectively, and thus $\beta\Delta G_{\rm crit} \simeq 31.2$, 19.4, 13.7, $R_{\rm crit}/\sigma \simeq 24.7$, 19.4, 16.3, and $n_{\rm crit} \simeq 1524$, 738, 438. Hence, CNT gives reasonable predictions for the barrier height. In addition, we find good agreement of $R_{\rm crit}/\sigma$ with the elongations $r^*_{\rm max}/\sigma \sim 20$ (see Fig. 4) and $\sim$16 obtained from simulations for $\Delta P^* = 0.052$ and 0.062, respectively. However, CNT overestimates dramatically $n_{\rm crit}$. The theory can be improved by taking into account the ellipsoidal shape of the cluster and the anisotropy of the interfacial tension.

In conclusion, we have developed a new cluster criterion that allows us to follow for the first time the IN transition. Applying this criterion, we find spinodal decomposition as well as nucleation and growth in accordance with the experimental observation of both phenomena in solutions of boehmite rods [5], F-actin [2], clay rods [3], and on mixtures of rodlike viruses and polymer [1,4]. In addition, this cluster criterion enables us to determine the height of the nucleation barrier and to study the shape and size of the nematic clusters. Our results show that the critical cluster size is many times smaller than the experimentally observed tactoids. This suggests that the "long-lived and stable" tactoids that are observed experimentally are postcritical and are in a late stage of the phase separation, i.e., the tactoidal growth regime. We hope that our findings stimulate new experiments on the nucleation process, which is present at an earlier stage of the phase separation. CNT overestimates the number of rodlike particles in the critical nucleus, which calls for better nucleation theories for anisotropic particles. We note that our cluster criterion opens up a whole new field in which the kinetics of many other phase transitions of anisotropic particles can be studied, including transitions in molecular fluids and isotropic-smectic transitions of short hard rods and of attractive rods, for which recent experiments show intriguing phenomena such as surface-induced smectic phases on nematic tactoids, smectic membranes winding off from tactoids as twisted ribbons, and melting of lamellar phases [1,15].

We thank E. Sanz and R. van Roij for useful discussions. This work was financially supported by the Nederlandse Organisatie voor Wetenschappelijk Onderzoek (NWO).

[1] Z. Dogic and S. Fraden, Phil. Trans. R. Soc. A **359**, 997 (2001); Z. Dogic, Phys. Rev. Lett. **91**, 165701 (2003).
[2] J. Viamontes *et al.*, Phys. Rev. Lett. **97**, 118103 (2006).
[3] Z. X. Zhang and J. S. van Duijneveldt, J. Chem. Phys. **124**, 154910 (2006).
[4] M. P. Lettinga *et al.*, J. Phys. Condens. Matter **17**, S3609 (2005).
[5] M. P. B. van Bruggen *et al.*, Macromolecules **32**, 2256 (1999).
[6] P. R. ten Wolde *et al.*, Phys. Rev. Lett. **75**, 2714 (1995).
[7] S. Auer and D. Frenkel, Nature (London) **409**, 1020 (2001); **413**, 711 (2001).
[8] P. R. ten Wolde and D. Frenkel, Science **277**, 1975 (1997).
[9] T. Schilling and D. Frenkel, Comput. Phys. Commun. **169**, 117 (2005); Phys. Rev. Lett. **92**, 085505 (2004).
[10] P. G. Bolhuis and D. Frenkel, J. Chem. Phys. **106**, 666 (1997).
[11] C. Dellago *et al.*, Adv. Chem. Phys. **123**, 1 (2002); P. G. Bolhuis *et al.*, Annu. Rev. Phys. Chem. **53**, 291 (2002).
[12] P. Prinsen and P. van der Schoot, Phys. Rev. E **68**, 021701 (2003).
[13] Z. Y. Chen and J. Noolandi, Phys. Rev. A **45**, 2389 (1992).
[14] A. Poniewierki and J. Stecki, Mol. Phys. **38**, 1931 (1979).
[15] A. M. Alsayed *et al.*, Phys. Rev. Lett. **93**, 057801 (2004).